Anisochemical Homopolymer/Diblock Copolymer Thin Film Blends

Michael D. Smith and Peter F. Green*

Department of Chemical Engineering, Texas Materials Institute, The University of Texas at Austin, Austin, Texas 78712

Randall Saunders

Sandia National Laboratories, Albuquerque, New Mexico 87185

Received May 28, 1999; Revised Manuscript Received October 4, 1999

ABSTRACT: We examined the effect of the addition of homopolymers tetramethylbisphenol A polycarbonate, TMPC, and poly(norbornene−methyl-d_3-carboxylate), NBMC, on the interlamellar spacing and the phase stability of symmetric poly(styrene-*b*-methyl methacrylate) diblock copolymer thin films on silicon substrates. The films were of thickness h, $L < h < 5L$, where L is the interlamellar spacing of the microphase separated PS-*b*-PMMA diblock copolymer. The homopolymers considered had degrees of polymerization, N_{TMPC} and N_{NBMC}, comparable to one-half of the degree of polymerization of the diblock. In the TMPC/diblock blend, for low TMPC homopolymer concentrations, $\varphi_{TMPC} < 0.2$, the homopolymer chains were localized in the middle of the PS micro-ordered domains, and the interlamellar spacing increased as $L/(1 - \varphi_{TMPC})$. For $\varphi_{TMPC} > 0.2$ the morphology of the diblock copolymer changed to accommodate higher volume fractions of TMPC. This behavior is contrasted with earlier observations in the PS-*b*-PMMA/PS homopolymer system where this diblock accommodated considerably higher PS homopolymer volume fractions while maintaining a lamellar phase. In the NBMC/diblock system the interlamellar spacing increased as $L/(1 - \varphi_{NBMC})$ for homopolymer concentrations up to $\varphi_{NBMC} \approx 0.05$. For $\varphi_{NBMC} > 0.05$, the NBMC formed a pure layer on the substrate, with the diblock maintaining its microphase separated structure on this layer. These results are discussed in light of mean field theory and in terms of the effect of the interfacial constraints on the phase behavior.

Introduction

Polymer thin films play a critical role in several applications such as protective coatings, adhesives, and sensors. In each of these cases, a fundamental understanding of issues related to blend thermodynamics and interfacial properties is critical for reliable materials design and performance. In recent years, many theoretical and experimental studies have addressed the problem of how the phase behavior of A/B thin film polymer blends is affected by the additional interactions with and restrictions imposed by both the substrate and the free surface on the blend constituents.[1−17]

For a bulk A/B homopolymer mixture, the phase behavior is determined by a combination of the translational entropy of the chains and the enthalpic interactions between the two components, represented by the Flory−Huggins segmental interaction parameter, χ.[18] When this mixture is confined to a thin film on a substrate, however, the presence of the solid substrate and free surface introduce additional effects that stem from the interactions between the constituents of the blend, the free surface, and the substrate. The component with the lower surface energy will be preferentially attracted to the free surface if the interfacial energetics have a larger contribution to the free energy than the entropic contributions such as chain stiffness and disparity in degrees of polymerization.[16,17] The component with the lower interfacial energy with the substrate will be attracted there. Additionally, the conformations of the polymer chains near the substrate and free surface are affected. This preferential adsorption of the chains at the interfaces modifies the symmetry of the bulk phase diagram.[12]

There is an additional effect observed in thin films. Computer simulations of blends confined between neutral surfaces show that the mixture becomes stabilized with confinement.[9,12,17] In addition, independent experiments by Reich and Cohen showed that the thin film geometric constraint increased the lower critical solution temperature, LCST, with decreasing film thickness of a polystyrene/poly(vinyl methyl ether) blend on a gold substrate, thereby improving the stability of the system to phase separation.[3] Thus, both the symmetry of the phase diagram and the phase stability of the mixture are affected when an A/B homopolymer blend is confined between two interfaces.

In a recent publication, Orso and Green examined a thin film mixture of symmetric diblock poly(styrene-*b*-methyl methacrylate) with homopolystyrene on silicon.[19] In this system, the diblock forms alternating PS-rich and PMMA-rich lamellae parallel to the substrate. They showed that the thickness of the diblock layer in contact with the substrate, L_1, which is equal to one-half the interlamellar spacing for a pure diblock, remains insensitive to swelling with the addition of PS homopolymer. For homopolystyrene with molecular weight comparable to the molecular weight of the PS diblock component, the homopolymer preferentially segregated to the center of the PS domains, whereas low molecular weight homopolymer chains were more uniformly distributed throughout the PS domains. Moreover, they showed that the domains incorporated a higher fraction of homopolymer chains than a comparable bulk system while retaining the lamellar structure. In essence, transitions from the lamellar phase to other ordered phases are frustrated. When the homopolymer content exceeded the solubility limit, the excess PS homopolymer macrophase separated, forming a separate layer at the free surface.

10.1021/ma9908494 CCC: $18.00
Published on Web 11/20/1999

In this paper we investigate in further detail the manner in which the phase morphology of thin film blends of homopolymers with diblock copolymers is determined by a combination of (i) homopolymer/copolymer enthalpic interactions, (ii) entropy associated with the distribution of the homopolymers into the copolymer domains, and (iii) the free surface and substrate interactions with the constituents of the blend.

Two cases are examined. The first homopolymer/diblock copolymer blend analyzed was tetramethylbisphenol A polycarbonate, TMPC, homopolymer, with PS-*b*-PMMA. The bulk TMPC/PS binary homopolymer system exhibits a LCST, and the two components are completely miscible for all concentrations at the temperature considered, 180 °C.[20] Bulk samples of TMPC and PMMA are incompatible. In the second case, we considered the PS-*b*-PMMA diblock mixed with poly(norbornene−methyl-d_3-carboxylate), NBMC, homopolymer. Binary mixtures of NBMC/PS and NBMC/PMMA are incompatible at this temperature, as we show later.

Experimental Section

PS-*b*-PMMA diblock copolymer having total molecular weight $M = 65\,500$ ($M_{PS} = 33\,000$, $M_{PMMA} = 32\,500$; $N_{PS} \approx 317$, $N_{PMMA} \approx 325$) and polydispersity index $M_w/M_n < 1.06$ was purchased from Polysciences, Inc. We also used TMPC homopolymer with weight-average molecular weight $M = 37\,900$ ($N_{TMPC} \approx 129$) and $M_w/M_n < 2.77$ as well as NBMC homopolymer having weight-average molecular weight $M = 26\,379$ ($N_{NBMC} \approx 174$) and $M_w/M_n < 1.025$. The NBMC was synthesized by living ring-opening metathesis polymerization (ROMP) of 5-norbornene-2-methyl-d_3-carboxylate.[21]

Solutions were made of TMPC and PS-*b*-PMMA in toluene with homopolymer volume fractions, φ, ranging from 0.01 to 0.25. Solutions of NBMC and PS-*b*-PMMA were similarly made with φ from 0.025 to 0.12. Films were made using a photoresist spinner to coat the solutions on silicon wafers having a native oxide layer approximately 20 Å thick. The surfaces of the as-spun films were smooth. The films were subsequently scored and annealed, under vacuum, at 180 °C for times in excess of 24 h. Twenty-four hours is far in excess of the time required for the topographical features to develop.

When a symmetric PS-*b*-PMMA diblock film orders on a substrate, steps are seen at the edge of the film.[19] The steps are the result of the multilayered, PS-rich and PMMA-rich, lamellar domains, of spacing L, oriented parallel to the substrate. A PMMA-rich layer is located at the substrate, and a PS-rich layer is located at the free surface. Because a different component lies at either interface, the height of the layer in contact with the Si substrate is of thickness $L/2$.[22−30] The height of subsequent steps is of a characteristic length, L, corresponding to the interlamellar spacing of the micro-ordered domains. Additionally, terraces of height L, islands or holes, appear on the surface of the ordered diblock film as dictated by the commensurability between the interlamellar spacing and the thickness of the film. The islands and holes appear on the surface if the local thickness of the film, t, is not exactly equal to $(n + {}^1/_2)L$, where n is an integer. In this case, the excess material not used to create a completely uniform layer forms the islands and holes at the surface. The islands, holes, and steps are characteristic of the lamellar morphology. These features are not observed in asymmetric block copolymers that do not form lamellar morphologies.[22]

The topographical analysis of our samples was performed using an Autoprobe CP (Park Scientific) atomic force microscope, AFM. The edges and surfaces of the homopolymer/diblock copolymer blend films were imaged in numerous locations in order to obtain accurate values for the interlamellar spacing for the various homopolymer blend concentrations. Measurements of the edge also provided independent measurement of the film thickness. The initial, as-spun, film thicknesses were also measured by spectroscopic ellipsometry. Both measurements were in agreement.

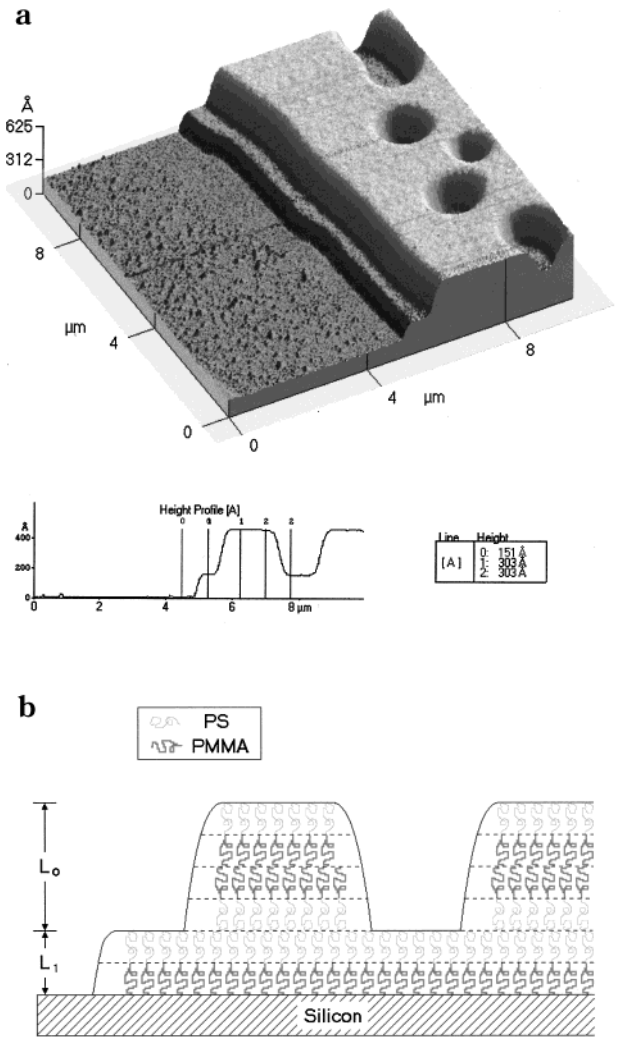

Figure 1. (a) Steps and surface features that develop at the edge of an ordered diblock copolymer film of PS-*b*-PMMA on silicon when the edge is scratched and the film annealed above T_g. (b) Simplified schematic of the orientation of the ordered diblock chains.

Supplemental analysis of an NBMC/PS-*b*-PMMA sample was performed by secondary ion mass spectroscopy, SIMS. Depth profile data was obtained using a Physical Electronics 6650 dynamic quadrupole SIMS. The primary ions were 1 kV O_2^+, rastered over areas ranging from 200 × 200 to 400 × 400 μm, and secondary ions were accepted from the center 20% of the craters. Charge neutralization was achieved using a static, defocused 2500 V electron beam.

Results

Figure 1a shows a scan of a PS-*b*-PMMA film. The average step height in this pure diblock is $L_0 = 303$ Å, and the height of the layer in contact with the substrate is $L_1 = 151$ Å. A schematic representation of this ordered diblock film on a silicon substrate is shown in Figure 1b to illustrate the general arrangement of the chains in the interior.

We now consider the mixture of TMPC homopolymer and the PS-*b*-PMMA diblock copolymer. A typical AFM scan of the surface of a film containing 10% TMPC homopolymer is shown in Figure 2. The domain spacing, $L = 338$ Å, is obtained from AFM line scans of these surface features as well as the steps at the edge of a film. A plot showing the interlamellar spacing, L, as a

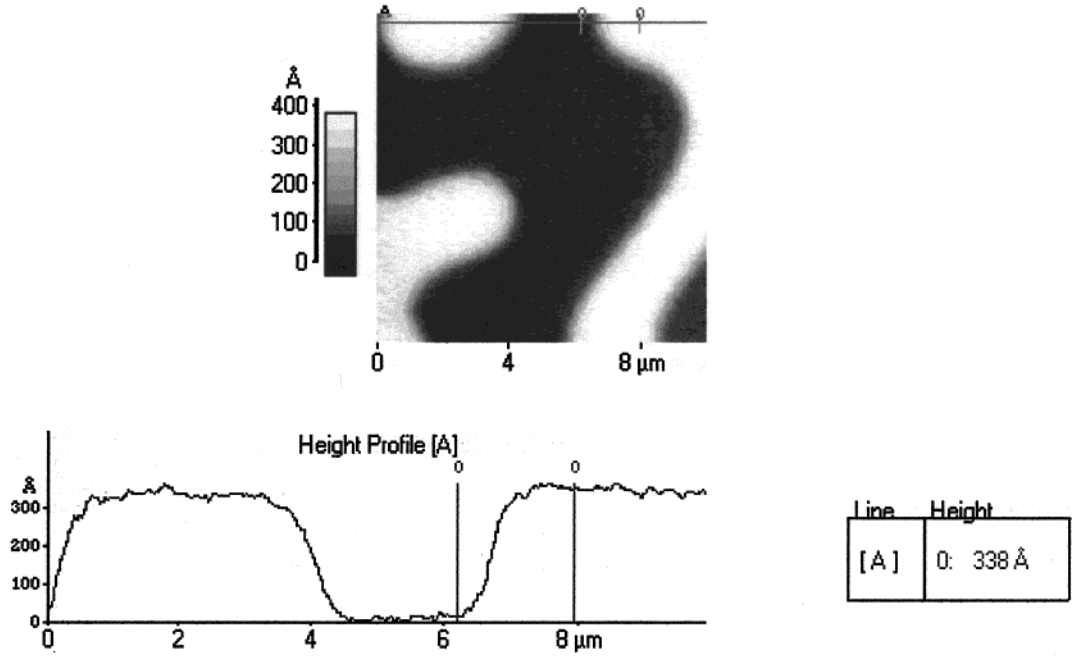

Figure 2. AFM scan of surface features having height L for a film of TMPC homopolymer blended with PS-*b*-PMMA diblock, $\varphi = 0.10$.

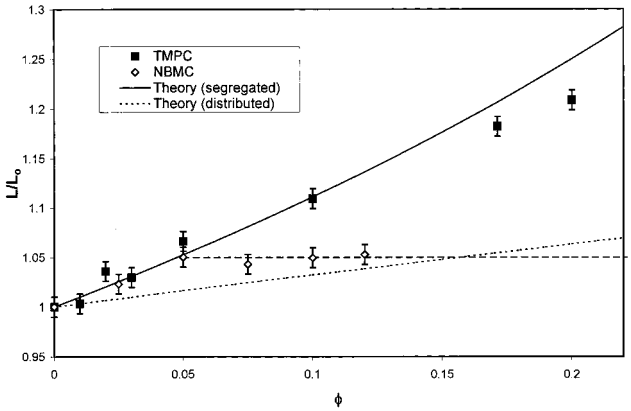

Figure 3. Homopolymer concentration dependence on the interlamellar spacing for blends of TMPC and NBMC homopolymers with PS-*b*-PMMA diblock copolymer. φ is a measure of the volume fraction of homopolymer in the spun film, not necessarily the fraction of homopolymer in the diblock domains. The solid line (eq 1) represents the behavior of homopolymer segregated at the center of the domains, and the dotted line (eq 2) describes homopolymer distributed throughout the domain. The broken line corresponds to $L/L_0 = 1.05$.

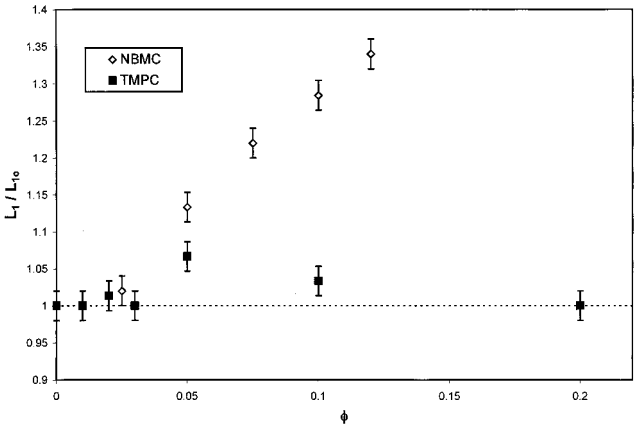

Figure 4. L_1 is plotted as a function of the homopolymer volume fraction.

function of the volume fraction of homopolymer, φ, is shown in Figure 3. It is evident from this plot that addition of TMPC homopolymer causes the interlamellar spacing to swell. At lower homopolymer concentrations, the swelling is well described by the solid line, whereas it deviates slightly for $\varphi > 0.15$. Figure 4 shows the dependence of the thickness of the copolymer layer in contact with the substrate, L_1, on the volume fraction of added homopolymer. This layer, which is $L_1 \approx 0.5L_0$ for the pure diblock, remains insensitive to swelling with increasing homopolymer content.

If we turn our attention now to the second blend involving NBMC homopolymer with PS-*b*-PMMA, we note from Figure 3 that the NBMC homopolymer also swells the diblock microdomains, though not nearly to the degree of the TMPC homopolymer. These data show that at small φ the increase is well described by the solid line. When $\varphi > 0.05$, L becomes independent of φ. The broken line in Figure 3 serves to emphasize the fact that L is constant for $\varphi > 0.05$. We observe from Figure 4 that L_1 increases significantly in this system for $\varphi > 0.05$. Figure 5 shows a representative scan of the edge of a film containing 12% NBMC homopolymer. It is evident from this scan just how much this layer adjacent to the substrate has grown. The reason for this large increase in L_1, which differs greatly from that caused by PS or TMPC homopolymers, is discussed later.

Discussion

The two components of an A-b-B diblock copolymer melt, at temperatures below the order−disorder transition temperature, T_{ODT}, will phase separate to reduce the number of unfavorable A/B contacts, thereby minimizing the free energy of the system. Because the two phases are chemically joined, they are unable to macrophase separate and instead microphase separate into A-rich and B-rich ordered domains. Ordered diblock systems can form several different morphologies, including lamellae, spheres, hexagonally packed cylinders, and bicontinuous double-diamond structures.[31] The

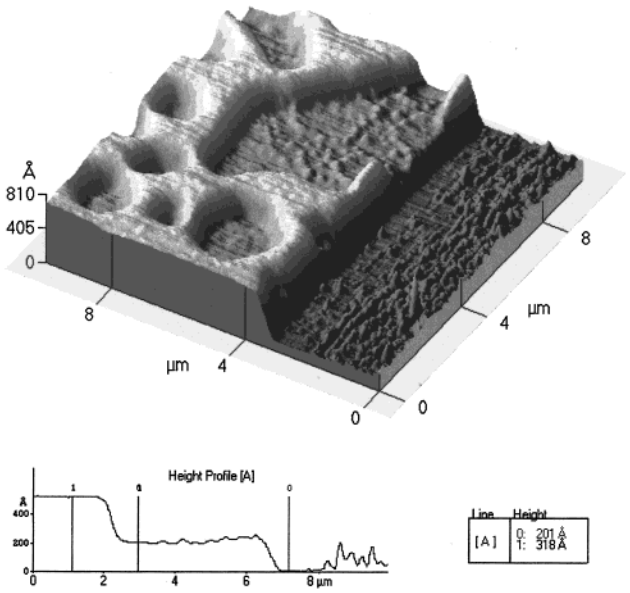

Figure 5. Image of the edge of a blend of 12% NBMC homopolymer.

particular phase structure the system adopts will depend on χ, on the number of segments per copolymer chain, and on the relative volume fraction of each phase. Since our copolymer is symmetric, it forms a lamellar morphology.

If we now consider an A or B homopolymer blended with a symmetric A-b-B diblock copolymer thin film on a substrate, we find that the phase behavior is influenced by the relative molecular weights of the components.[32−50] If the molecular weight of the homopolymer is significantly less than that of the appropriate diblock component, the homopolymer chains intermingle with the diblock chains, and the homopolymer is distributed throughout the diblock domain (Figure 6a). This is the so-called "wet brush" case discussed by Leibler.[25] Conversely, if the homopolymer is of comparable molecular weight to the diblock component, the homopolymer segregates to the middle of the corresponding diblock component microdomains (Figure 6b). The driving force behind this phase behavior is a competition between translational and conformational entropy. For short homopolymer chains, the increase in translational entropy associated with allowing the chains to intermingle outweighs the slight decrease in conformational entropy resulting from the stretching of the copolymer chains to make room for the homopolymer. For the longer chains, however, the diblock chains would have to stretch appreciably to allow the homopolymer chains to intermingle, resulting in a substantial decrease in the conformational entropy of the diblock chains, much more than would be gained from any increase in translational entropy of the homopolymer chains. Since in this case the copolymer "brush" layers would not be interpenetrated by the homopolymer, this situation would correspond to the so-called "dry-brush" condition.[25]

Hamdoun et al. proposed a theoretical prediction for the behavior of nanosized inorganic particles incorporated into an ordered diblock copolymer.[24] Their model assumes a consistent lamellar ordered morphology but is not specific to the type of species blended with the diblock. Orso and Green showed that these theoretical predictions also describe the behavior of an A/A-b-B

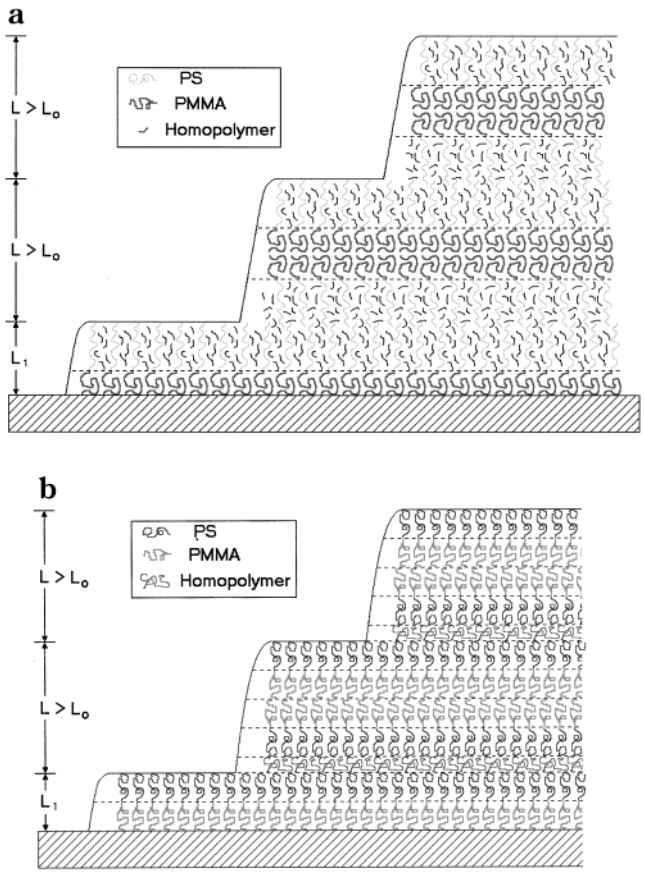

Figure 6. A simplified representation of a cross section of the edge of a film of (a) PS-*b*-PMMA diblock blended with low molecular weight PS homopolymer when the added homopolymer is distributed uniformly throughout the PS microdomains and (b) PS-*b*-PMMA diblock blended with high molecular weight PS homopolymer when the added homopolymer is localized at the center of the PS domains.

blend.[19] If the added material is localized in the middle of the ordered microdomains, then the interlamellar spacing is given by

$$L_{\text{localized}} = L_0/(1 - \varphi) \tag{1}$$

where L_0 is the interlamellar spacing of the pure diblock, and φ is the volume fraction of the homopolymer in the sample. As illustrated in Figure 6b, when the homopolymer chains are localized at the center of the domains, the diblock components remain relatively unperturbed, so the microordered domains swell significantly as more homopolymer is added.

If, however, the homopolymer is more uniformly distributed within the A domain of the diblock, then Hamdoun et al. predict

$$L_{\text{distributed}} = \frac{L_0/[g(f,\varphi)]^{-1/3}}{1 - \varphi} \tag{2}$$

where

$$g(f,\varphi) = \frac{f + (1 - f)\varphi^2}{f(1 - \varphi)^2}$$

Here, f is the volume fraction of the A component in the diblock copolymer. f is $^1/_2$ for a symmetric diblock. As illustrated in Figure 6a, if the homopolymer chains are uniformly distributed throughout the A domain, the

intermingling of the chains will cause the A diblock chains to stretch axially (perpendicular to the substrate) and also to swell laterally (parallel to the substrate). This lateral swelling increases the area per copolymer junction, which necessitates a shrinking of the B domain in order to maintain uniform density throughout the film. The increase in the swelling of the A domain offsets the shrinking of the B domain, and the net result is an increase in the interlamellar spacing, though not as large as for the previous case, $L_{\text{localized}} > L_{\text{distributed}} > L_0$.

These equations are the source of the theoretical predictions that appear in Figure 3. The solid line corresponds to the domain swelling if the homopolymer chains are localized in the middle of the appropriate domain, as described by eq 1, and the dotted line represents the domain spacing if the homopolymer chains are uniformly distributed throughout the appropriate domain, as described by eq 2.

We now consider the blend of TMPC homopolymer with the PS-*b*-PMMA diblock copolymer. In this blend, the domain swelling data of Figure 3 show that the interlamellar spacing increases with added homopolymer. The degree to which the domains swell seems to be well described by eq 1, for homopolymer concentrations $\varphi < 0.12$, indicating that the TMPC homopolymer chains are initially being localized in the center of the PS domains, as we would expect from the relative size of the homopolymer chains. We can conclude that it is the PS domains that incorporate the TMPC homopolymer because of the favorable enthalpic interactions between the two components. We also note, from Figure 4, that L_1 is relatively insensitive to the addition of TMPC homopolymer. That the thickness of the first layer is $L_1 = L_0/2$ indicates that PMMA remains at the substrate and PS at the free surface. A value of $L_1 = L$ would indicate that the same component existed at both interfaces. This is clearly not the case. Studies of binary mixtures of PS and TMPC show that PS always segregates to the free surface, indicating that the surface energy of PS is smaller than that of TMPC.[51] Hence, TMPC remains confined within the copolymer.

The morphology of films with TMPC concentrations $\varphi > 0.15$ changed, and the well-defined features showing island, holes, and steps gradually disappeared. Samples with TMPC concentrations greater than 20% became unstable; they ruptured and dewet, exposing the substrate. Figure 7 shows the morphology of a sample that dewet. In this sample, one edge of the film was scored to expose the substrate so that we could use it as a reference. The line scan shows that the bare substrate has been exposed between the droplets. Note that as a result of dewetting the amount of surface area of PS exposed to the free surface has increased because the system went from a layered structure to droplets. Note further that in the ordered system all the A/B copolymer interfaces were flat in order to minimize the number of unfavorable A/B contacts. Dewetting increased these unfavorable A/B interactions. Clearly, the system underwent a change in morphology in order to accommodate the TMPC. This new structure is obviously not lamellar. A detailed investigation of the morphology of this structure is beyond the scope of this paper and will have to be addressed at a later time.

The behavior of the NBMC/PS-*b*-PMMA system is very different. From an analysis of binary mixtures, PS/NBMC and PMMA/NBMC, we observed that NBMC phase separates into bilayers when combined with

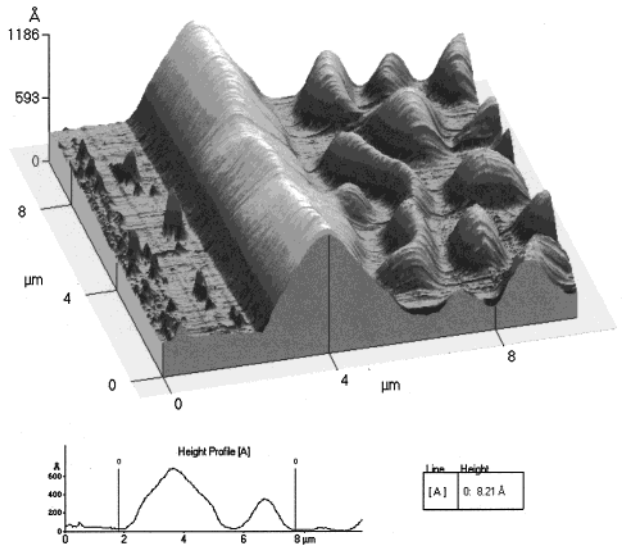

Figure 7. A three-dimensional AFM image of a PS-*b*-PMMA/TMPC film that dewet a silicon substrate at 180 °C after 24 h. The left of the image shows the surface of the silicon. Polymer was scratched from that region.

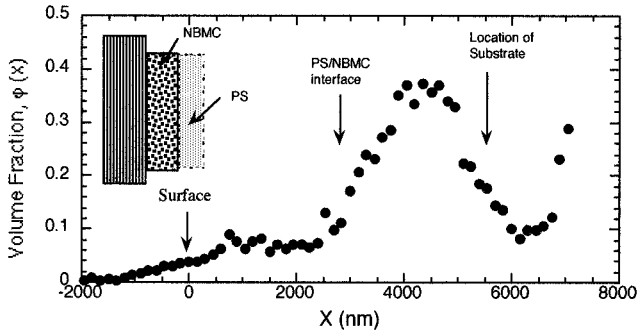

Figure 8. A volume fraction versus depth profile of deuterated NBMC in a PS/NBMC blend is shown here. The system forms a bilayer after annealing at 180 °C for 2 h. A layer of PS forms at the free surface. This profile was obtained using FRES.

either PS or PMMA homopolymer. Figure 8 shows the volume fraction versus depth profile of deuterated NBMC in a PS/NBMC blend annealed for 2 h at 180 °C. The profile of this film of thickness 500 nm was determined using forward recoil spectrometry.[52] The profile shows that the NBMC segregated to the substrate. The polystyrene is located at the free surface. These data indicate that NBMC has a higher surface energy than PS and a lower interfacial energy with the substrate. Similar observations were also made for PMMA/NBMC blends.

We now examine the effect of the NBMC homopolymer on the PS-*b*-PMMA diblock. From Figure 3, we note that the interlamellar spacing increases with added NBMC homopolymer, but only for $\varphi < 0.05$. For $\varphi > 0.05$ adding more homopolymer to the diblock has no effect on the interlamellar spacing. Additionally, we note from Figure 4 that L_1 increases drastically for $\varphi > 0.05$.

To gain a better understanding of the phase behavior of this system, we examined a sample using dynamic secondary ion mass spectroscopy, SIMS. The result of such a scan on a sample containing 7.5% NBMC is shown in Figure 9. The solid line tracks the deuterium present in the NBMC, and the broken line measures the silicon. This SIMS analysis indicates that the majority of the NBMC is localized at the substrate, but some of the homopolymer is present in the diblock. From

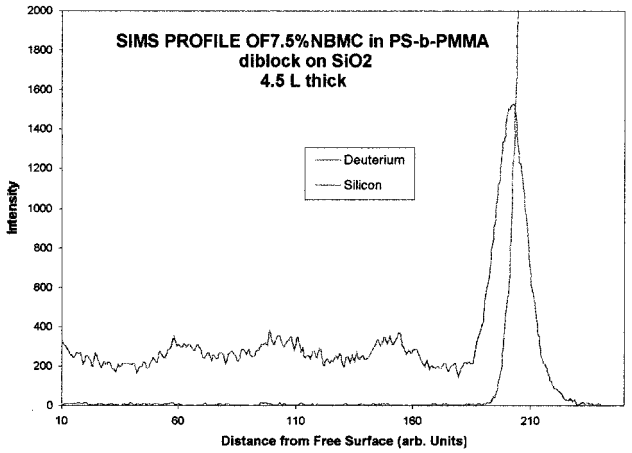

Figure 9. SIMS depth profile of a 7.5% NBMC/PS-*b*-PMMA blend. The film is of thickness $t \approx 4.5L$.

an AFM scan of the same sample we can determine that the film is $4.5L$ thick. Knowing this, we can compare the SIMS data to a known model of how the PS-*b*-PMMA diblock orders and thereby conclude that some of the NBMC is incorporated in the PMMA domains. Thus, despite forming bilayers in a binary mixture, NBMC displays some degree of solubility in the ordered PMMA diblock domains.

It therefore seems that, for very small homopolymer concentrations, the NBMC chains are predominantly localized at the center of the PMMA ordered domains. However, once the solubility limit has been exceeded, $\varphi > 0.05$, NBMC chains rapidly form a separate phase at the substrate/copolymer interface. NBMC has a lower interfacial energy with silicon than PMMA, explaining the fact that the NBMC forms its separate phase at the substrate. It is now clear that the L_1 measured and plotted in Figure 4 actually includes this layer of pure NBMC at the substrate with the $L_0/2$ diblock layer ordered on top of it. The fact that the diblock layer in contact with the NBMC layer is of thickness $L = L_0/2$ confirms that NBMC has a greater affinity for PMMA, and it truly is the PMMA domains that incorporate the NBMC homopolymer. If NBMC had a greater affinity for PS, then L_1 would be greater than L in the blend. These data also tell us independently that NBMC has a higher surface energy than PS. This is expected on the basis of the FRES measurements of the NBMC/PS system.

Conclusions

We showed that the phase morphology of thin film blends of homopolymers with symmetric diblock copolymers is determined by a combination of the homopolymer/copolymer segmental interactions and by the interactions between the constituents of the blend and the substrate and free surface.

We observed that TMPC chains of comparable degree of polymerization to a block constituent do not interpenetrate the dense brush layers. Instead, the chains segregate to the middle of the PS domains, thereby increasing the domain size with increasing TMPC volume fraction, φ. The domain spacing increased as $L_0/(1 - \varphi)$, where L_0 is the initial domain size. The favorable enthalpic contributions together with the gain in translational entropy that would favor miscibility of the block-PS/TMPC chains (interpenetration of the copolymer brush) appear to be outweighed by contributions due to the conformational entropy penalty associated with that process. Confinement to the middle of the block-PS domains is evidently more favorable. For higher volume fractions of TMPC, beyond 0.16, the topographical features of the sample changed, indicating a gradual change in the microstructure to accommodate the TMPC. For $\varphi_{TMPC} > 0.2$, the system became unstable.

In contrast, the weakly interacting homopolymer, NBMC, exhibited limited miscibility in the PMMA domains. At low NBMC volume fractions, the swelling of the layers was consistent with $L = L_0/(1 - \varphi)$. At higher volume fractions, $\varphi > 0.05$, the NBMC preferentially segregated to the silicon substrate. The diblock copolymer formed an ordered lamellar structure on the layer of NBMC at all compositions beyond $\varphi = 0.05$. This NBMC layer increased in thickness with increasing φ. It is noteworthy that our earlier experiments with PS homopolymer chains of comparable degree of polymerization to the PS component of the block had the same effect on the interlamellar spacing; L increased as $L_0/(1 - \varphi)$. When the solubility limit of PS was reached, the PS homopolymers phase separated toward the free surface of the ordered copolymer.

It would appear that if the homopolymer chains do not strongly interact with either of the copolymer constituents, then they would phase separate to the free surface or substrate, depending on the interfacial interactions, and the copolymer would remain ordered without a change in morphology. In the case of PS-*b*-PMMA/TMPC, the TMPC had a strong preferential affinity for PS. It had a weaker affinity for the free surface and for the substrate. Under these conditions, the copolymer structure underwent a substantial change to accommodate the homopolymer.

Acknowledgment. This work was supported by the National Science Foundation (DMR-9705101). We thank T. Mates of the University of California at Santa Barbara for performing SIMS measurements. M. Smith acknowledges partial support from the Bob West Endowed Graduate Fellowship in Engineering and from the Texas ATP program.

References and Notes

(1) Schmidt, I.; Binder, K. *J. Phys. (Paris)* **1985**, *46*, 1631.
(2) Rouanault, Y.; Baschnagel, J.; Binder, K. *J. Stat. Phys.* **1995**, *80*, 1009.
(3) Reich, S.; Cohen, Y. J. *Polym. Sci., Polym. Phys. Ed.* **1981**, *19*, 1255.
(4) Brudkowski, A.; Steiner, U.; Klein, J. *J. Chem. Phys.* **1992**, *97*, 5229.
(5) Bruder, F.; Brenn, *Phys. Rev. Lett.* **1992**, *68*, 1326; *Europhys. Lett.* **1993**, *22*, 707.
(6) Steiner, U.; Klein, J.; Fetters, L. *J. Phys. Rev. Lett.* **1994**, *72*, 1498.
(7) Jones, R. A. L.; Norton, L. J.; Kramer, E. J.; Bates, F. S.; Wiltzius, P. *Phys. Rev. Lett.* **1991**, *66*, 1326.
(8) Heier, J.; Kramer, E. J.; Revesz, P.; Battistig, G.; Bates, F. S. *Macromolecules* **1999**, *32*, 3758.
(9) Tang, H.; Szeilfer, I.; Kumar, S. K. *J. Chem. Phys.* **1994**, *100*, 5367.
(10) Green, P. F.; Christensen, T. M.; Russell, T. P.; Jerome, R. *J. Chem. Phys.* **1990**, *92*, 1478.
(11) Hariharan; Kumar, S. K.; Rafailovich, M. H.; Sakolov, J.; Zeng, X.; Doung, D.; Schwartz, S.; Russell, T. P. *J. Chem. Phys.* **1993**, *99*, 656.
(12) Flebbe, T.; Dunweg, B.; Binder, K. *J. Phys. II* **1996**, *6*, 667.
(13) Geoghegan, M.; Jones, R. A. L.; Sivia, D. S.; Penfold, J.; Clough, A. S. *Phys Rev. E* **1996**, *53*, 825.
(14) Genzer, J.; Kramer, E. *J. Phys. Rev. Lett.* **1997**, *78*, 4946.

(15) Sung, L.; Karim, A.; Douglas, J. F.; Han, C. C. *Phys. Rev. lett.* **1996,** *76*, 4368.
(16) Wu. D.; Fredrickson, G. H.; Leibler, L. *J. Polym. Sci. B* **1995** *33*, 2323.
(17) Kumar, S. K.; Tang, H.; Szeilfer, I. *Mol. Phys.* **1994**, *81*, 867.
(18) de Gennes, P.-G. *Scaling Concepts in Polymer Physics*; Cornell University Press: London, 1979.
(19) Orso, K. A.; Green, P. F. *Macromolecules* **1999**, *32*, 1087.
(20) Guo, W.; Higgins, J. S. *Polymer* **1990**, *31*, 699.
(21) Saunders, R. A. *Macromolecules* **1995**, *28*, 4347.
(22) Karim, A.; Singh, N.; Mohan, M.; Bates, F. S. *J. Chem. Phys.* **1994**, *100*, 1620.
(23) Ausserre, D.; Raghunathan, V. A.; Maaloum, M. *J. Phys. II* **1993**, *3*, 1485.
(24) Hamdoun, B.; Ausserre, D.; Cabuil, V.; Joly, S. *J. Phys. II* **1996**, *6*, 503.
(25) Leibler, L. *Makromol. Chem. Macromol. Symp.* **1988**, *16*, 1.
(26) van Dijk, M. A.; van den Berg, R. *Macromolecules* **1995**, *28*, 6773.
(27) Gadegaard, N.; Almdal, K.; Larsen, N. B.; Mortsen, K. *Appl. Surf. Sci.* **1999**, *142*, 608.
(28) Mayes, A. M.; Russell, T. P.; Satija, S. K.; Majkrzak, C. F. *Macromolecules* **1992**, *25*, 6523.
(29) Walton, D. G.; Kellogg, G. J.; Mayes, A. M.; Lambooy, P.; Russell, T. P. *Macromolecules* **1994**, *27*, 6225.
(30) Mayes, A. M.; Russell, T. P.; Deline, V. R.; Satija, S. K.; Majkrzak, C. F. *Macromolecules* **1994**, *27*, 7447.
(31) Bates, F. S.; Fredrickson, G. H. *Annu. Rev. Phys. Chem.* **1990**, *41*, 525.
(32) Whitmore, M. D.; Noolandi, J. *Macromolecules* **1985**, *18*, 2486.
(33) Banaszak, M.; Whitmore, M. D. *Macromolecules* **1992**, *25*, 2757.
(34) Hong, K. M.; Noolandi, J. *Macromolecules* **1983**, *16*, 1083.
(35) Winey, K. I.; Thomas, E. L.; Fetters, L. J. *Macromolecules* **1991**, *24*, 6182.
(36) Winey, K. I.; Thomas, E. L.; Fetters, L. J. *Macromolecules* **1992**, *25*, 2645.
(37) Winey, K. I.; Thomas, E. L.; Fetters, L. J. *J. Chem. Phys.* **1991**, *95*, 9367.
(38) Zin, W. C.; Roe, R. J. *Macromolecules* **1984**, *17*, 183.
(39) Roe, R. J.; Zin, W. C. *Macromolecules* **1984**, *17*, 189.
(40) Matsen, M. W. *Macromolecules* **1995**, *28*, 5765.
(41) Tanaka, H.; Hasegawa, H.; Hashimoto, T. *Macromolecules* **1991**, *24*, 240.
(42) Hashimoto, T.; Tanaka, H.; Hasegawa, H. *Macromolecules* **1990**, *23*, 4378.
(43) Hashimoto, T.; Shibayama, M.; Kawai, H. *Macromolecules* **1983**, *16*, 1093.
(44) Tucker, P. S.; Barlow, J. W.; Paul, D. R. *Macromolecules* **1988**, *21*, 2794.
(45) Tucker, P. S.; Paul, D. R. *Macromolecules* **1988**, *21*, 2801.
(46) Lowenhaupt, B.; Steurer, A.; Hellmann, G. P. *Macromolecules* **1994**, *27*, 908.
(47) Adedeji, A.; Hudson, S. D.; Jamieson, A. M. *Polymer* **1997**, *38*, 737.
(48) Xie, R.; Yang, B.; Jaing, B. *J. Polym. Sci., Polym. Phys. Ed.* **1995**, *33*, 25.
(49) Xie, R.; Yang, B.; Jaing, B. *J. Polym. Sci., Polym. Phys. Ed.* **1996**, *34*, 1489.
(50) Winey, K. I.; Thomas, E. L.; Fetters, L. J. *Macromolecules* **1992**, *25*, 422.
(51) Kim, E.; Kraush, G.; Kramer, E. J. *Macromolecules* **1994**, *27*, 5927.
(52) Green, P. F.; Doyle, B. L. Ion beanm analysis of thin polymer films. In *New Characterization Techniques for Thin Polymer Films*; Tong, H. M., Nguyen, L.T., Eds.; Wiley: New York, 1990.

MA9908494